This is a repository copy of *Mitigating drilling-induced damage and hot-wet aging effects through reconsolidation in CF/PEKK composites*.

White Rose Research Online URL for this paper:
https://eprints.whiterose.ac.uk/id/eprint/227185/

Version: Published Version

eprints@whiterose.ac.uk
https://eprints.whiterose.ac.uk/

Original Manuscript

Mitigating drilling-induced damage and hot-wet aging effects through reconsolidation in CF/PEKK composites

Sinem Elmas[1,2], Buse Atac[1,2], Abdulrahman Al-Nadhari[1,2], Serra Topal[1,2,3], Mehmet Yildiz[1,2] and Hatice S Sas[1,2,4]

Abstract

This study investigates the impact of reconsolidation on the mechanical properties and damage recovery of carbon fiber reinforced poly ether ketone ketone (CF/PEKK) composites caused by manufacturing processes, particularly drilling, and environmental aging. Reconsolidation is performed using a hot-press method on both reference and aged composite samples. Mechanical properties are evaluated through compression and open-hole compression (OHC) tests, leveraging the digital image correlation (DIC) technique for deformation analysis. Additionally, thermal properties are characterized using dynamic scanning calorimetry (DSC), thermogravimetric analysis (TGA), and dynamic mechanical analysis (DMA). Before aging, compressive strength increases by 15.61% in compression samples and by 37.61% in OHC samples due to reconsolidation process. This recovery is further supported by enhancements in the glass transition temperature (T_g) and degree of crystallinity (X_c) by 5.97% and 20.94%, respectively. After aging, the compressive strength of the reconsolidated samples is slightly lower than that of the aged reference samples, yet still shows significant improvements in mitigating aging effects and reducing catastrophic failures. The DIC analysis further confirms that reconsolidation reduces delamination and catastrophic failures, confirming the reconsolidation process's efficacy in restoring mechanical integrity and performance.

[1]Faculty of Engineering and Natural Sciences, Sabanci University, Orhanli-Tuzla, Istanbul, Turkey
[2]Integrated Manufacturing Technologies Research and Application Center, Sabanci University, Orhanli-Tuzla, Istanbul, Turkey
[3]Research and Innovation Center for Graphene and 2D Materials (RIC2D), Khalifa University, Abu Dhabi, United Arab Emirates
[4]School of Mechanical, Aerospace and Civil Engineering, The University of Sheffield, Sheffield, UK

Corresponding author:
Hatice S Sas, School of Mechanical, Aerospace and Civil Engineering, The University of Sheffield, Sheffield, S1 3JD, UK.
Email: h.s.sas@sheffield.ac.uk

Introduction

Thermoplastic matrix composites (TPCs) gain interest in the aviation, automotive, and energy sectors due to their outstanding properties including reparability, excellent resistance, weldability, and high chemical resistance.[1,2] Among various thermoplastic matrix materials, the Poly Aryl Ether Ketone (PAEK) family stands out as a suitable candidate for use in the aviation industry due to its high performance and superior properties.[3] Poly ether ketone ketone (PEKK), which belongs to the PAEK family, is prominent in structural applications within the aerospace sector due to its relatively lower processing temperature compared to poly ether ether ketone matrix (PEEK),[4] as well as its better matrix ductility and higher strength.[5]

The vacuum-bag-only (VBO) process is a promising out-of-autoclave (OoA) manufacturing method that offers a cost-effective and time-efficient alternative to traditional autoclave processing. While it has the potential to produce high-quality thermoplastic composites (TPCs), existing literature on its manufacturing challenges and optimization strategies remains limited. Zhang et al.[6] investigate the void reduction mechanisms during oven VBO (vacuum bag-only) processing of thermoplastic composites (TPCs), highlighting the significance of interlayer permeability and edge conditions for process success. This relationship is particularly crucial for thick composite laminates, where these factors have a substantial impact on void reduction effectiveness. In another study, Zhang et al.[7] report that air removal during VBO processing of TPCs can be modeled as a combination of through-thickness gas diffusion and in-plane airflow within the interlayer region. Similarly, Swamy et al.,[8] demonstrate that various VBO setup conditions are crucial for advanced TPC manufacturing to achieve effective void removal, resulting in efficient consolidation and low void content.

During the operational life of aircraft, damages can occur due to mechanical impact and environmental conditions, as well as during the manufacturing and assembly stages of the composite structure. Voids, micro-cracks, and delamination are some examples of manufacturing-related damages.[9] Additionally, the mechanical joining of large-sized composite structures with other composites and metal parts may be necessary at the assembly stage. In order to perform operations such as riveting, screwing, and bolted joining during assembly, drilling is an indispensable machining process on the composite structure.[10,11] Drilling is a material removal process that creates holes progressively through composite layers using a rotary cutting tool.[12] In carbon fiber-reinforced thermoplastic composites like CF/PEKK, the heterogeneous microstructure and the high thermal stability of the reinforcing fibers make the material particularly susceptible to damage during drilling. Common defect modes include delamination, matrix smearing, fiber pull-out, and thermal degradation, all of which are highly sensitive to process

parameters and material morphology.[10,12,13] While most composite drilling studies to date have focused on conventional thermoset systems such as CF/epoxy[14] recent research has started to address the unique challenges associated with drilling thermoplastic composites. Ge et al.[15] are among the first to systematically compare different hole-making methods for CF/PEKK, revealing that conventional drilling introduces more severe microstructural damage compared to helical milling. They also have observed an increase in matrix crystallinity, attributed to strain-induced crystallization triggered by elevated temperatures and shear stress during drilling. In a follow-up study, the same group has conducted a multi-objective optimization of the CF/PEKK drilling process,[14] offering key parametric recommendations for minimizing damage and promoting sustainable manufacturing of next-generation thermoplastic composites.

Moreover, aircraft are subjected to various environmental conditions throughout their service life, such as humidity, moisture, high temperature, rain erosion, hail, lightning strikes, and ultraviolet radiation, all of which contribute to material degradation.[16–18] The damage occurring in composite structures under various loading conditions during operation accelerates due to these environmental factors. The most critical environmental factor is temperature change, with hot-wet environments being particularly detrimental to composite performance.[19,20] Hydrothermal aging, which results from hot-water absorption, can trigger certain damage types like the debonding of the matrix/fiber interface, or in other words, delamination, through the effects of plasticization, molecular degradation, and swelling of the polymer matrix, consequently leading to catastrophic failure.[19–22] Given that environmental conditions and exposure time differently affect composite performance and service life, it is critical to understand the behavior of composites under these conditions. Accelerated aging analyses provide an important and cost-effective means of predicting long-term material performance.[23,24] However, there are limited studies in the literature that explore the impact of hot-wet environments on advanced thermoplastic composites. Batista et.al.[25] investigate the hygrothermal conditioning effects on the degree of crystallinity and mechanical properties of CF/PEEK composites. They have subjected the samples to hygrothermal conditioning in a climate chamber at 80°C and 90% relative humidity for about 8 weeks until saturation, finding that the samples gain 0.14% weight with an increase in degree of crystallinity due to polymer chain relaxation and reordering. They also observe increases in compressive strength and Young's modulus, suggesting that the fiber–matrix interface is not degraded by moisture absorption. Moreover, Mazur et al.[26] presented a study on the influence of accelerated aging on the compression and shear properties of CF/PEKK composites. Their study involves conditioning composite samples at 80°C and 90% RH for about 6 weeks until reaching a saturation point with a weight gain of ∼0.22%. Their findings report significant enhancements in the compression and shear properties, indicating an anti-plasticization effect. In addition, our previous work has identified the following effects: (i) the impact of void content on the alteration of failure mechanisms in in situ consolidated CF/PEKK composites,[9] (ii) the influence of AFP lay-up process parameters and lay-up defects, such as gaps and overlaps, on mechanical performance,[27] and (iii) the effect of micro- and meso-defects on tensile performance of glass-fiber reinforced epoxy composites, and all three with corresponding failure mode transformations under

hydrothermal aging conditions.[17] However, there is still a lack of studies in the literature addressing the recovery, namely repair, of these defects, particularly those introduced by micro-cracks and drilling, both with and without hydrothermal aging conditions.

Thermoplastic matrices have the ability to soften and melt with heat and pressure and then solidify again allowing the repair of damaged areas.[28] Reconsolidation proves to be a remarkable method in which damage such as voids, cracks, and delamination is recovered by leveraging the melting-solidification nature of TPCs through the aid of heating and applying pressure. Ragupathi et al.,[29] demonstrated a complete recovery of the cracked and separated layers with the mechanical properties in terms of tensile strength remaining 89% similar to the reference samples by applying ultrasonic reconsolidation to CF/PEEK samples. It is worth noting that the significant impact of the reconsolidation process on mechanical properties is studied in existing literature. Conejo et al.[30] have studied the reconsolidation effect on the CF/PAEK composite samples subjected to impact energies of 5, 10, and 30 J, followed by compression after impact (CAI) testing. Their findings indicate that after reconsolidation using a hot press, the compression strength of the sample impacted at 5 J impact energy return to the same strength value as the reference sample, while samples impacted with 10 J and 30 J exhibit partial recovery. Essentially, the basis for the improvement in mechanical properties achieved through reconsolidation is the elimination of residual stresses. Residual stresses arise from several causes such as shrinkage in thermoplastic polymers, processing conditions (e.g. cooling rate), elastic properties, and, the mismatch between the coefficient of thermal expansion of matrix and fiber, causing them to expand or shrink at different rates when exposed to elevated temperatures during manufacturing or operation.[31] During reconsolidation, the controlled heating and cooling process helps relieve and redistribute these residual stresses, which were induced by the loads and environmental conditions experienced by the aircraft.[31,32] Additionally, various studies in the literature aim to recover the mechanical properties of the composites that are exposed to environmental factors throughout their lifetime. To eliminate the aging effect and improve mechanical properties, Erklig et al.[33] have examined the effects of hydrothermal aging and subsequent drying on glass fiber/epoxy samples. After exposure to hydrothermal aging at 25°C, then fully dry them at 50°C until constant weight and conduct Charpy impact tests. Consequently, the wet samples show a 27.3% decrease, while the re-dried samples experience only a 2.60% decrease in impact strength compared to the reference sample.

The mechanism and effects of damage occurring during the drilling of the composites are challenging and not predictable. To the best of the authors' knowledge, studies on reducing and/or eliminating these effects and enhancing mechanical properties are limited in the literature. Nonetheless, in the study of Borba et al.,[34] two composites are joined using a friction-riveted application, where the heat generated by friction leads to the reconsolidation of the PEEK matrix. This process reduces the notch effect, which is a type of damage commonly seen in conventional lock-bolted joint applications, consequently enhancing the load-bearing capacity. Despite the great potential of the reconsolidation process for thermoplastic composites (TPCs), there is a lack of comprehensive efforts that demonstrate the repair success in: (i) recovering the effects of aging, (ii) eliminating the deteriorative impact of the drilling process, and (iii) addressing the combined damage

caused by both drilling and aging. Building on these insights, our current work seeks to fill this critical gap by exploring repair strategies for defects, particularly those caused by micro-cracks and drilling, under both hydrothermal aging and non-aging conditions.

The objective of this study is to first present a reconsolidation process recipe using heat and pressure for advanced TPCs, aiming to mitigate damages incurred during environmental aging and/or drilling. As part of the study, samples undergo drilling for OHC testing, and selected samples are subjected to hydrothermal aging at 70°C for 1000 hours in distilled water. Subsequently, all samples undergo to the reconsolidation process in a hot press. Compression and OHC tests are conducted to evaluate the effects of aging and reconsolidation, utilizing the DIC technique to monitor full-field deformation. Additionally, void content and thermal analyses, including DSC, TGA, and DMA, are performed to assess the microstructural and thermal properties of CF/PEKK composites manufactured by the VBO process and the reconsolidated thermoplastic composites.

Materials and experimental methods

Materials

The CF/PEKK unidirectional tape with a nominal thickness of 0.15 mm and a width of 305 mm (Toray Cetex®TC1320) is supplied by Toray Advanced Composites, USA. It has a fiber areal weight of 145 g/m^2, a prepreg areal weight of 221 g/m^2, with a resin content of 34 % by weight.

Manufacturing of composite laminates

Quasi-isotropic CF/PEKK composite laminates, with a configuration of $[45/0/-45/90]_{3s}$ and dimensions of $((110 \times 310 \times 3.15) \pm 0.1)$ mm, are manufactured using the VBO process. The VBO manufacturing lay-up and oven cycle are illustrated in Figure 1. A release agent (Loctite Frekote 700-NC) is applied to a steel plate before the lay-up process. UPILEX® 25S, a polyimide perforated release film, and woven glass fabric Bleeder Lease® E-peel ply with 0.107 mm thickness are positioned on the top and bottom of the tape stacking, respectively. (Figure 1(a) and (b)). This arrangement enhances air removal to reduce void content and prevents bonding between the laminate and tooling materials.[35] Airweave® UHT800, a nonwoven ultra-high temperature fiberglass breather, is then placed on top of the perforated release film to aid in air evacuation and maintain vacuum levels. The stack is finally covered with Thermalimide E polyimide film and securely sealed using A-800 3G sealant tape, preparing it for placement in the oven. The vacuum bag lay-up is placed in the oven, and a vacuum is set at 1 atmosphere (atm) and maintained at a consistent pressure for a 24-h debulking process at room temperature (Figure 1(c)). After debulking, the oven temperature is raised to 250°C at a heating rate of 4°C/min, and further increased to 378°C at a heating rate of 3°C/min while maintaining the pressure at 1 atm[35] (Figure 1(e)). The laminates are held at this elevated temperature for a dwell period of 90 minutes,[8] and then gradually cooled to room temperature at a rate of 3°C/min. The VBO-manufactured CF/PEKK samples are designated as
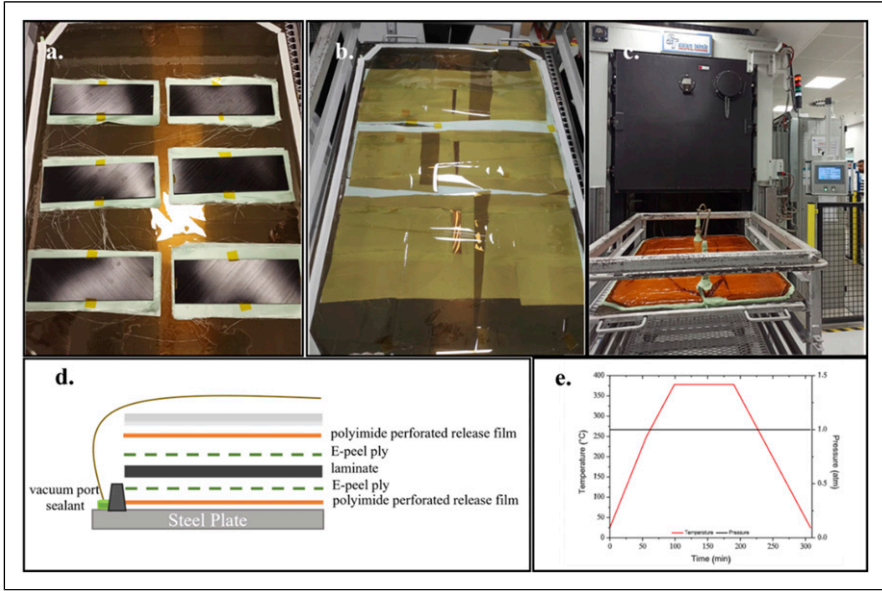
Figure 1. VBO manufacturing of CF/PEKK laminates. (a) Lay-up, (b) Lamination, (c) Oven consolidation, (d) Schematic illustration of VBO process, (e) Oven temperature and pressure cycle.

"Reference_BA" (Before Aging). Finally, the composite laminates are cut using a water jet (KUKA—KR 16–2C-F) in accordance with the specified standards for character-ization and the holes are drilled by using a 3-axis computer numerical control (CNC) laser cut machine (POYSAN B54-90).

The fiber volume content analysis is carried out with three repeats according to ASTM D3171/Method B using samples in the dimensions of (25 × 25) mm, to find void ratio of the composite laminates, which undergo matrix digestion with a mixture of sulfuric acid (H_2SO_4) and hydrogen peroxide (H_2O_2) treatment. The void content is calculated using equation (1)[36]:

$$V_v = 100 - (V_f + V_m) \text{ with } V_f = \frac{M_f}{M_i} x \frac{\rho_i}{\rho_f} x100 \text{ and } V_m = \frac{M_i - M_f}{M_i} x \frac{\rho_i}{\rho_m} x100 \quad (1)$$

where V_f, V_m, and V_v are the volumetric percentages (%) of the fibers, matrix, and voids in the composite accordingly. M_f, and M_i are the mass (g) of the sample after digestion, and the mass of the sample before digestion. ρ_f, ρ_m and ρ_i are the densities (g/cm³) of the fibers, matrix, and the CF/PEKK composite sample, respectively. ρ_f and ρ_m are 1.79 and 1.30 g/cm³, according to the supplier data sheet.[37,38] The density of composite laminate ρ_i is determined as 1.57 g/cm³ according to ASTM D792/Method A, utilizing water buoyancy in accordance with Archimedes' principle.

Accelerated hydrothermal aging of CF/PEKK samples

The hydrothermal aging is carried out according to ASTM D5229 standard by using 3 repetitions of the composite samples to assess the impact of heat and water on the composite samples. Initially, samples are dried in a 100°C oven for 24 h to remove any moisture absorbed during the water jet cutting process. Subsequently, these samples are weighed (M_0) before being subjected to accelerated hydrothermal aging. The accelerated hydrothermal aging tests are conducted by immersing CF/PEKK samples in distilled water at 70°C for 1000 h.[25,27] The reference CF/PEKK samples, which have undergone aging, is named "Reference_AA". The samples are regularly weighed throughout to aging process to determine the water uptake content. The average water uptake content (M) is then calculated using equation (2):

$$M(\%) = \frac{M_w - M_0}{M_0} \times 100 \qquad (2)$$

where M_w is the aged average weight of the sample (g), and M_0 is the average dry weight of the sample (g).

When the samples reach the saturation point, they are subsequently reconsolidated in a hot press to prevent any moisture loss during the process. This step ensures that the samples retain their absorbed moisture content, allowing for a more controlled and consistent evaluation of their behavior under the specified conditions.

Reconsolidation process

Reconsolidation is carried out using a hot press process which is an effective and economical process, by MSE Hot Press LP_A4SH50_450 to mitigate the effects of drilling and hydrothermal aging, thereby enhancing the load-bearing capacity of the samples. The hot press process is a more efficient method for reconsolidation since it reduces the need for consumables, streamlining the procedure and reducing both processing time and complexity. A frame is used during the hot press process, with the samples placed symmetrically to ensure uniform laminate thickness and prevent any reduction in thickness during reconsolidation. Thermalimide E polyimide film is placed on the bottom and upper surfaces of the plate to prevent the composites from sticking (Figure 2(a)). For the reconsolidation process, the composite laminates are initially heated from room temperature to 380°C under 1 bar of pressure, with a heating rate of 10°C/min to improve heat transfer efficiency. Once the target temperature is reached, the pressure is increased to 10 bar and maintained for 30 minutes to facilitate reconsolidation. Finally, the laminates are cooled at a rate of 10°C/min until room temperature is reached (Figure 2(b)). This process is adapted from the literature, as summarized in Table S1.[30,39–43] No resin bleeding or thickness reduction is observed after the reconsolidation process, with the final reconsolidated laminates maintaining a thickness of 3.15 mm. The CF/PEKK samples that undergo the reconsolidation process before aging are labeled as "Reconsolidated_BA," while those reconsolidated after the aging period are labeled as "Reconsolidated_AA."
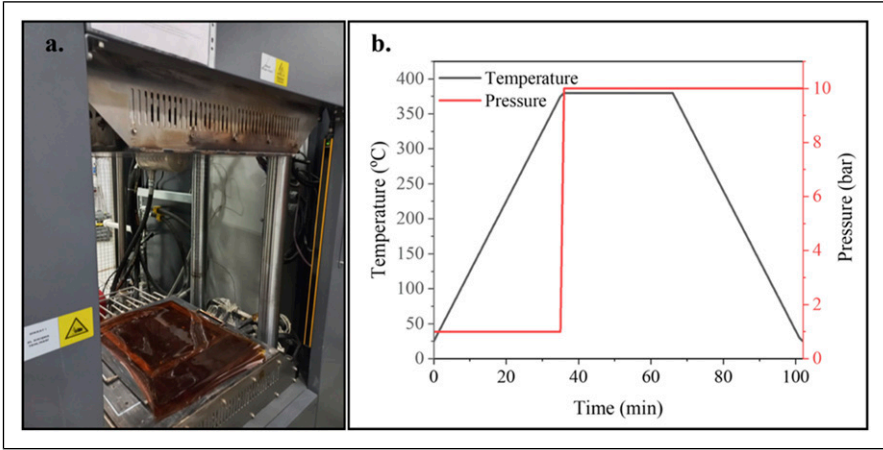
Figure 2. Reconsolidation process: (a) Hot-press set up, (b) Temperature, and pressure cycle.

Thermal characterization

Thermal characteristics are determined through DSC and TGA. DSC analysis is employed to evaluate the thermal properties of VBO-manufactured CF/PEKK composite laminates and study the impact of hydrothermal aging and reconsolidation on various properties, including T_g, melting temperature (T_m), crystallization temperature (T_c), melting/crystallization enthalpies, and X_c. DSC measurements are conducted using the Mettler Toledo DSC^{+3} analysis instrument with hermetic aluminum pans. Composite samples approximately 25 mg in mass (corresponding to dimensions of $(4 \times 4) \pm 0.1$ mm), are analyzed within a temperature range of 25°C–400°C, employing a heating/cooling rate of 10°C/min under an inert nitrogen (N_2) atmosphere with a flow rate of 50 mL/min. The findings are evaluated by Mettler Toledo DSC+3 STARe SW16.30 software. The X_c is calculated according to equation (3) by comparing the melting enthalpy of the composite to the melting enthalpy of PEKK material with 100% crystallinity ($\Delta H^0_m = 130$ J/g)[44];

$$X_c = \frac{\Delta H_m}{\Delta H^0_m \times W_m} \times 100 \qquad (3)$$

where ΔH_m is the melting enthalpy obtained from DSC measurement, and W_m is the matrix weight fraction in the composite sample. The W_m is obtained from fiber volume content analysis and equals to 35.84 %.

Thermal degradation analysis was performed using a composite sample of approximately 120 mg in mass (with dimensions of $(5 \times 5) \pm 0.1$ mm) via a Mettler Toledo TGA-DSC3 + apparatus to evaluate thermal stability. The temperature range investigated was 25°C–1000°C, with a heating rate of 10°C/min under N_2 atmosphere. DMA is conducted using the samples in the dimension of $((55 \times 13 \times 3.15) \pm 0.1)$ mm, according to the ASTM D7028-07 standard through Mettler Toledo DMA1 instrument in dual cantilever mode

following the ASTM D4065 standard. The analysis is performed over a temperature range of 25°C–250°C employing a heating rate of 3°C/min at a frequency of 1.00 Hz. All of the thermal analysis are repeated two times.

Mechanical characterization and damage monitoring

Compression tests are carried out to adhere to ASTM D6641 combined loading compression. The samples are in dimensions $((140 \times 13 \times 3.15) \pm 0.1)$ mm in height, width, and thickness, respectively. The glass fiber tabs in the dimensions of $((63.5 \times 13 \times 2) \pm 0.1)$ mm are uniformly bonded adhesively at the sample ends. Tests are carried out using the Instron 5982 Universal Testing Machine instrument with a 100 kN load cell. The crosshead speed is maintained at 1.3 mm/min throughout the tests.

The OHC test is carried out in accordance with ASTM D6484 with sample dimensions of 300 mm (length), 36 mm (width), and 6 mm (center hole diameter). Tests are performed on an Instron 5985 Universal Testing Machine equipment with a 100 kN load cell, and the crosshead speed is maintained at 2 mm/min throughout the tests. Each mechanical test is conducted three times.

Following the mechanical tests, microscopic observations of the fracture surfaces are conducted using Nikon—LV100ND microscopy to gather information on the damage mechanisms of quasi-isotropic CF/PEKK samples.

To monitor the full-field deformation of both compression and OHC samples throughout the entire testing process, the DIC technique is employed. Spackle patterns, applied with black and white spray paints with RAL codes 9005 and 9010 respectively, are textured onto the surfaces of the samples. Sensor calibration is conducted in single snap mode, following the manufacturer's specifications for a calibration object measuring (55×44) mm, with a working distance of 729 mm and a camera angle of 25°. Calibration deviations of 0.025 pixels (limit value: 0.050 Pixels) and a scale deviation of 0.001 mm (limit value: 0.005 mm) are achieved. Prior to mechanical testing, a reference measurement is taken in single-image mode. During the test, recorded data undergoes post-processing using ARAMIS professional software. Lagrangian strains of the spackle pattern on the samples are analyzed, with a facet size of 17 pixels and a point distance of 15 pixels. Figure 3 shows an example of the surface components created in ARAMIS to track the displacement vectors of compression (Figure 3(a)) and OHC (Figure 3(b)) samples.

Results and discussion

Void content analysis

Following the procedure outlined in previous section, M_f, and M_i are measured as 2.0112 g and 3.1345 g for the reference sample and, 2.0490 g and 3.1178 g, for reconsolidated sample, respectively in accordance with ASTM D3171/Method B. Subsequently, the void volume fractions are calculated as (0.34 ± 0.18) % and (0.50 ± 0.20) % for the reference and reconsolidated composite samples, respectively,
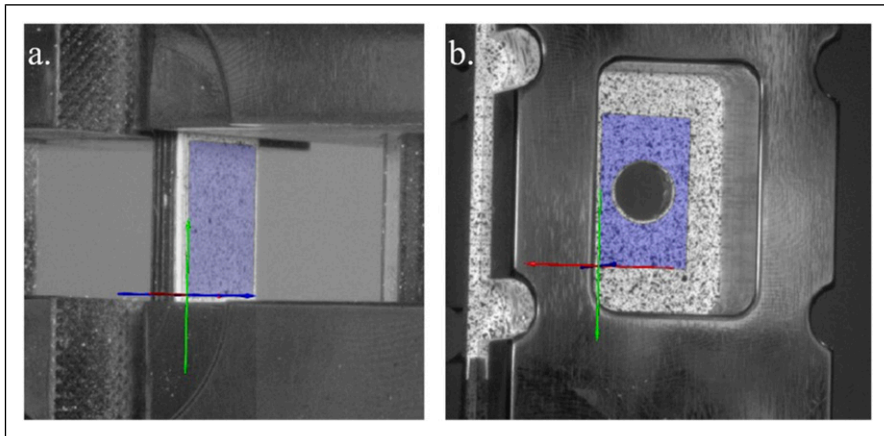
Figure 3. DIC technique implication and selected interest of region with white and black spackles for (a) Compression samples and (b) Open hole compression samples.

using equation (1). The void content is crucial for enhancing the mechanical properties and structural integrity of the composite, excessive void content can significantly weaken the structural integrity of the composite, leading to reduced mechanical properties and increased susceptibility to failure under load, the ratio of less than 1% is evidence of a successful manufacturing via VBO and reconsolidation process via hot-press.[45] The slight rise in void amount can be ascribed to reheating composites. However, this negligible increase indicates the successful outcome of the re-consolidation process in attaining desired void content levels, further confirms the effectiveness of the reconsolidation technique in improving composite properties.[46]

Hydrothermal aging results

The water uptake percentage of both compression and OHC samples as a function of time, calculated using equation (2), is shown in Figure 4. Both types of samples had a mass gain value of (0.26 ± 0.0025) wt.% and (0.23 ± 0.0014) wt.% after 1000 hours, respectively. This slight variation in mass gain values, namely water uptake percentages, can be attributed to differences in sample size and geometry. Initially, the water uptake percentage increases rapidly during the early stages of hydrothermal conditioning for both sample types. However, this increase is more pronounced in the OHC samples due to the central hole, which increases the area exposed to water. The drilling process introduces micro-damages around the hole, facilitating quicker water ingress, resulting in a more rapid initial water uptake for OHC samples compared to compression samples. After the initial period, the rate of increase slows until the end of the conditioning period. The mass gain results of all CF/PEKK samples in this study are consistent with the literature. Sukur et al.[27] has reported a similar water uptake trend, with a mass gain of 0.20 wt% for CF/PEKK composites manufactured using automated fiber placement. Moreover, Mazur
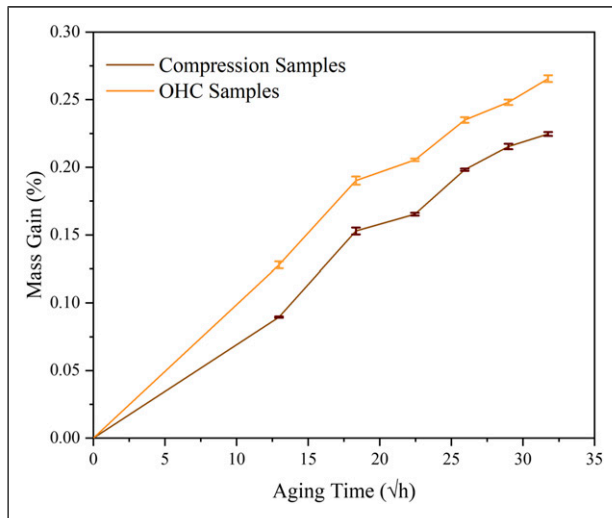
Figure 4. Mass gain (%) of the reference CF/PEKK composite samples as a function of the aging period.

et al.[26] indicates that CF/PEKK composite samples reached a saturation limit with a water absorption of approximately 0.22 % after 6 weeks of aging at 80°C and 90 % relative humidity (RH). Water absorption in polymer composites primarily occurs through diffusion from the sample surface, facilitated by microcracks, voids, or imperfections between the fiber and polymer matrix due to capillary action. Sukur et al.[9] has observed that increased void content levels (5.13 ± 0.38) % in composites led to a higher saturation value of 1.14 wt% after 30 days of hydrothermal aging. Moreover, water tends to penetrate the amorphous regions more than the crystalline regions of semicrystalline polymers. The absorbed plenty amount of water acts as a plasticizer, potentially lowering the T_g of thermoplastic polymers and leading to degradation in mechanical properties such as strength, modulus, and stiffness.[47] After the reconsolidation process, the mass of the hydrothermally aged samples decreases to near their initial states. Slange et.al.[48] have conducted ambient temperature conditioning (≈23°C/50% RH) on the CF/PEEK samples manufactured using hot press and AFP for 2 months to oven deconsolidation experiments. They observed a weight loss of approximately 0.3% for the AFP specimens and 0.08% for press-consolidated samples after oven deconsolidation at 390°C for 20 min. This decrease is attributed to the removal of absorbed water and some minor changes in material properties, such as density and the release of volatile components during heating.

Thermal characteristics

The heating and cooling curves of CF/PEKK samples before aging (BA) are shown in Figure 5(a) and (b), while those after aging (AA) are presented in Figure 5(c) and (d). The findings of the DSC analyses are summarized in Table 1. The T_g of the reference

composite is determined to be $(146.85 \pm 1.30)°C$ from the second heating curve, which increases by approximately 6.12% to $(155.84 \pm 1.17)°C$ after reconsolidation. Additionally, the reconsolidated sample exhibits a X_c of $(19.26 \pm 0.87)\%$, an improvement over the $(15.65 \pm 0.26)\%$, X_c of the reference sample, as calculated using equation (3). This increase in crystallinity can be attributed to chain segment migration and reordering during the reconsolidation process.[49,50] As a result, the increased area of the crystalline regions restricts the mobility of the amorphous regions, which in turn leads to a higher glass transition temperature (T_g) due to the more structured crystalline arrangement.[49] The melting enthalpy value of the sample increases after the 1000-h aging period, resulting in a crystallization degree of $(25.82 \pm 1.24)\%$. This enhancement is attributed to post-crystallization of the matrix, facilitated by temperature and water exposure. This process allows polymer chains in the amorphous regions to gain sufficient mobility, enabling them to reorient and recrystallize.[23] Consequently, an increase in the T_g is observed, reflecting the more ordered crystalline structure. A negligible change in thermal properties after aging suggests that reconsolidation does not significantly affect these properties. DMA is frequently used to characterize the viscoelastic properties, temperature dependence,
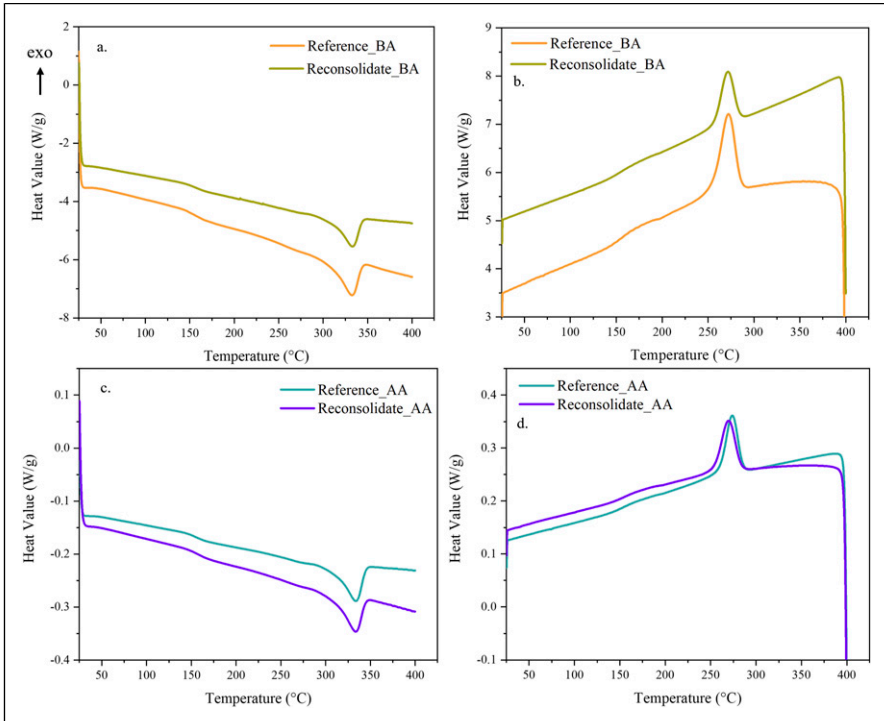

Figure 5. DSC results of reference and reconsolidated CF/PEKK composites: (a) Heating curve before aging, (b) Cooling curve before aging, (c) Heating curve after aging, and (d) Cooling curve after aging.

Table 1. Average values of thermal and thermo-mechanical results of reference and reconsolidate CF/PEKK composites before and after aging.

Sample	DSC			TGA		DMA			
	T_g (°C)	ΔH_m (J/g)	X_c (%)	T_d (°C)	Mass loss (%)	E' (GPa)	E'' (MPa)	E' onset (°C)	T_g (°C)
Reference_BA	146.85 ± 1.30	7.29 ± 0.12	15.65 ± 0.26	580.90 ± 2.90	12.40 ± 0.17	12.65 ± 1.55	632.97 ± 2.45	144.31 ± 4.30	141.30 ± 1.25
Reconsolidate_BA	155.84 ± 1.17	8.98 ± 0.41	19.26 ± 0.87	582.50 ± 2.38	12.44 ± 0.11	11.39 ± 1.16	531.18 ± 2.75	148.52 ± 4.58	161.15 ± 1.26
Reference_AA	155.05 ± 1.92	12.03 ± 0.58	25.82 ± 1.24	575.54 ± 2.87	13.79 ± 0.23	11.77 ± 1.78	519.82 ± 2.11	120.56 ± 4.76	158.51 ± 1.21
Reconsolidate_AA	157.15 ± 1.15	11.59 ± 0.43	24.88 ± 0.93	580.09 ± 2.88	12.67 ± 0.13	13.69 ± 1.27	560.17 ± 2.26	136.05 ± 5.08	156.76 ± 1.03

frequency dependence of modulus, transition temperatures more precisely. Therefore, the effects of aging and reconsolidation on T_g are discussed in greater detail and with enhanced sensitivity in the DMA results, as recommended in the literature.[51]

The thermograms from TGA analyses of CF/PEKK composites are presented in Figure 6. The major decomposition mechanism occurs at around 500°C to 680°C which is associated with random chain scission of the ether and ketone bonds.[52] It is noted that there is no significant change in the total mass loss and decomposition temperature (Td) between reference and reconsolidated CF/PEKK composite samples before aging process. This demonstrates that subjecting the material to a processing cycle shorter than first manufacturing cycle did not affect the thermal stability of the composite and therefore did not initiate decomposition. Nevertheless, after aging, there is a decrease in T_d from (580.90 ± 2.90)°C to (575.54 ± 2.87)°C and weight loss (%) is increased (Table 1). These results indicate a reduction in thermal stability following hydrothermal aging, as evidenced by lower temperatures corresponding to % weight loss. This decline in thermal stability is likely attributed to the synergistic effects of thermal and hydrolytic degradation.[53] However, it is observed that after hot-wet aging period, a subsequent reconsolidation process is led to reaching decomposition temperature and mass loss levels similar to those of the reference sample. This suggests that the thermal stability and mass loss characteristics of the material return to a state comparable to the original reference material after the reconsolidation process.

Thermomechanical behavior analysis

Figure 7 presents the DMA curves of the reference and reconsolidated CF/PEKK composite samples as a function of temperature, detailing the storage modulus (E′), loss modulus (E″), and tan(δ), both before and after aging. The findings are tabulated in Table 1. DMA is a sensitive technique that enables the study of polymeric chain relaxation, including determining parameters like the glass transition temperature and understanding how mechanical properties evolve during relaxation. The storage modulus
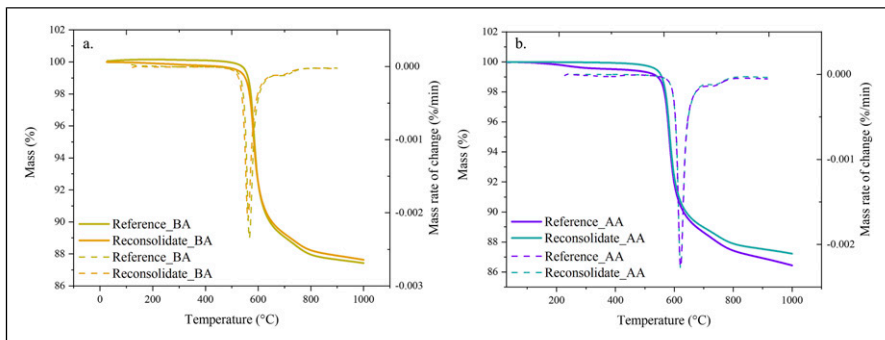

Figure 6. TGA (straight line) and DTG (dashed line) curves of reference and reconsolidate CF/PEKK composites: (a) Before aging and (b) After aging.

reflects the elastic response of a material, representing the energy stored and recovered during deformation, while the loss modulus indicates the viscous response, representing the energy dissipated as heat.[54] From the DMA results, it is observed that the storage modulus decreases from (12.65 ± 1.55) GPa to (11.39 ± 1.16) GPa (Figure 7(a)), and the loss modulus decreases from (632.97 ± 2.45) MPa to (531.18 ± 2.75) MPa (Figure 7(b))
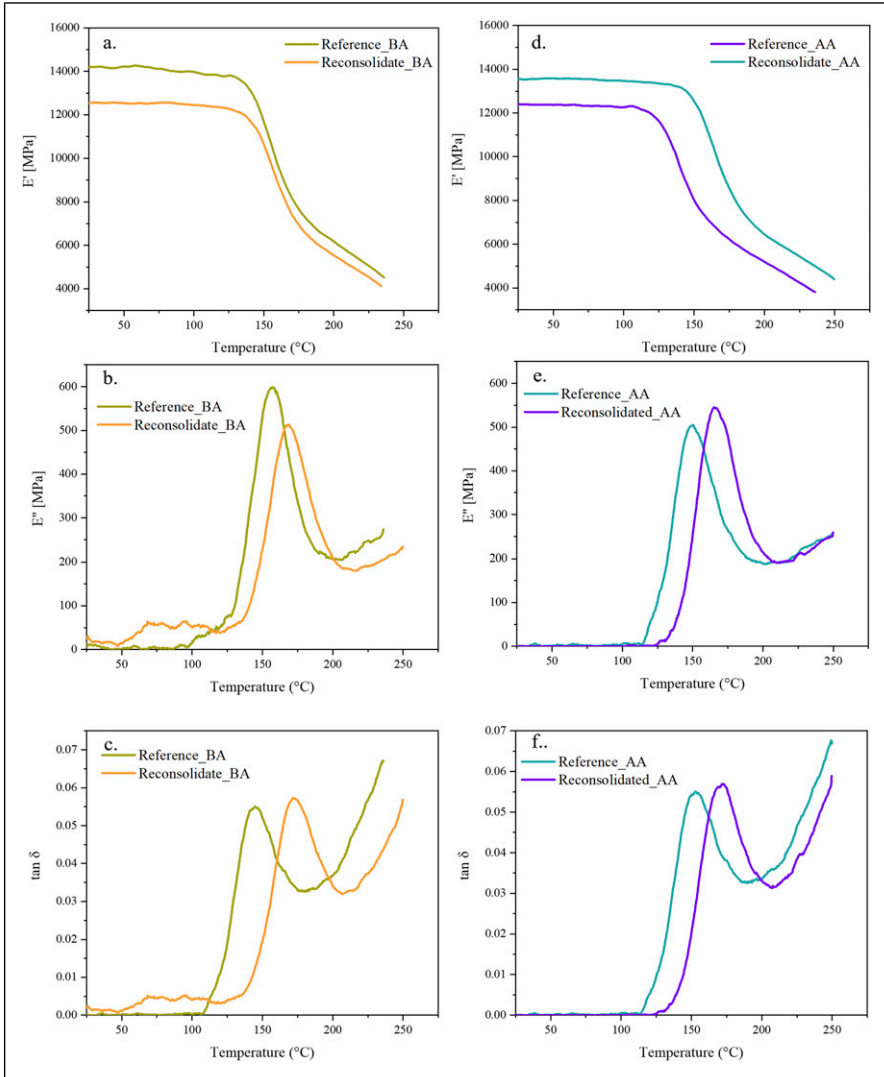

Figure 7. DMA curves of reference and reconsolidated CF/PEKK samples: (a and d) Storage modulus-temperature, (b and e) Loss modulus-temperature, and (c and f) Tan δ –temperature, before and after aging, respectively.

after the reconsolidation process for samples before aging. This reduction in modulus values is attributed to changes in the composite structure caused by the heat and pressure during reconsolidation. Since reference samples structure likely retained higher residual stress and stiffness, reconsolidation can relax and redistribute residual stresses, it may also lead to a decrease in modulus values.[31,55] Similarly, the decrease in the loss modulus after reconsolidation is due to the sample experiencing lower stress and thus requiring less energy input, reflecting a reduced viscous response and less energy dissipation as heat.[56] However, the onset of the transition temperature increases by 2.92% to $(148.52 \pm 4.58)°C$ compared to the reference sample (Figure 7(a) and (b)), indicating improved thermal stability. This behavior suggest that the material begins to deform and soften at a higher temperature.[57]

At the end of the 1000-h hot-wet aging period, the storage modulus (Figure 7(d)), loss modulus (Figure 7(e)), and the onset temperatures of transition decreased significantly compared to Reference_BA sample, as shown in Table 1. The onset temperature of storage modulus of the CF/PEKK sample decreased by 16.45 % from $(144.31 \pm 4.30)°C$ to $(120.56 \pm 4.76)°C$ (Figure 7(d)), demonstrating that the aging process reduces the service temperature limits of the material. The combined effect of moisture and water can initiate various degradation mechanisms, weakening interfacial adhesion strength between the fiber and matrix, ultimately reducing the storage modulus.[25] Following the aging period, the loss modulus decreases from (632.97 ± 2.45) MPa to (519.82 ± 2.11) MPa (Figure 7(e)), suggesting a reduction in the amorphous phase content within the CF/PEKK composite as it ages. This decrease can be attributed to an increase in the degree of crystallinity, likely resulting from post-crystallization through the structural rearrangement of PEKK as indicate in literature.[9] However, reconsolidation may have healed some micro-damages induced during the aging process, which counteracts the softening effects of aging.

The T_g values obtained from the tan (δ) graph (Figure 7(c) and (f)) are consistent with the DSC analysis results. The reconsolidation effect is particularly evident in samples that are not subjected to aging. After reconsolidation of the reference samples, the T_g value increased by 14.04 %, reaching (161.15 ± 1.26) °C. This increase confirms the enhancement of crystalline areas following the reconsolidation process, as explained in previous section, resulting in a more organized crystalline structure and, consequently, an observed increase in the T_g value.[49] The T_g of the CF/PEKK sample increased to $(158.51 \pm 1.21)°C$ after the 1000-h hot-wet aging period. The elevated temperature and moisture conditions enhance chain mobility in the amorphous region, leading to an increase in polymer crystallinity, often referred to as secondary crystallization. This process can result in the formation of new lamellae within the amorphous region, facilitated by the high temperature.[58,59] The slight decrease in T_g after reconsolidation can be attributed to a minor reduction in the degree of crystallization, as explained in the DSC results. However, this decrease is negligible, as the similar T_g values between the Reference_AA and Reconsolidate_AA samples indicate that the reconsolidation process effectively mitigates the effects of moisture uptake and temperature exposure. This recovery is due to the reformation of crystalline regions, aided by the applied temperature and pressure. Furthermore, the results from both DMA and DSC analyses confirm that the

thermoplastic material retains its thermal properties through reconsolidation process. The inherent ability of thermoplastic materials allows for the formation of crystalline lamellae during heating and cooling, demonstrating successful consolidation.

Mechanical test results

The compressive and open-hole compressive behavior of CF/PEKK samples are investigated to assess the effects of reconsolidation, including the impact of hydrothermal aging. The compressive performance of samples is evaluated with ASTM D6641 standard, following the Combined Loading Compression method. The compressive stress-strain curves of samples before and after aging are given in Figure 8. The VBO manufactured, Reference_BA sample is presented a compression strength of (489.94 ± 9.69) MPa that is compatible with literature results.[30] The compressive strength is increased to (576.72 ± 17.02) MPa by reconsolidation (Figure 8(a)). Additionally, the material's elastic region exhibited higher strain values compared to the reference sample. This improvement is attributed to the enhanced bonding quality between the fiber and matrix, defect closure due to pressure application during the reconsolidation process, and the effective reduction of residual stresses, all of which positively contribute to the mechanical properties of the composite material.[55] Upon comparing compression samples through microscopy investigation, it is observed that the delamination between layers, particularly in the central region, is reduced in the fracture area of the reconsolidated sample (Reconsolidate_BA) compared to the reference sample (Reference_BA), as shown in Figure 9(a) and (b). This reduction in delamination indicates increased resistance of the sample, contributing to its higher strength under compressive load.

After the hot-wet aging period, the compressive strength of the Reference_AA samples increased by 25.95% compared to the Reference_BA sample, reaching (617.09 ± 10.90) MPa (Figure 8(b)). This increase in compressive strength is attributed to post-crystallization reactions influenced by aging. However, water absorption has altered
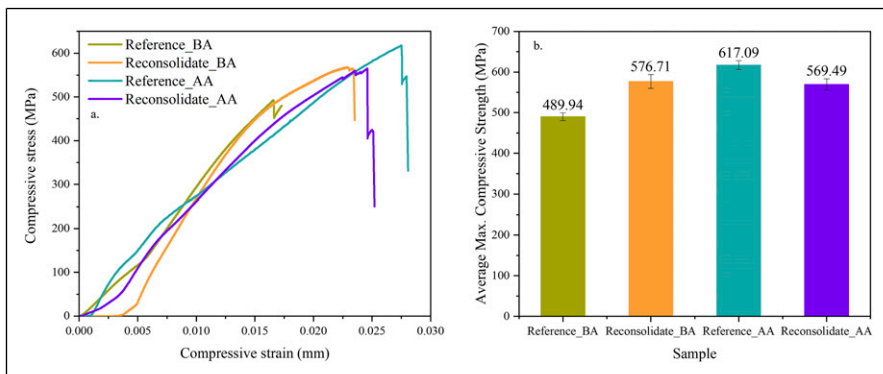

Figure 8. Compressive behavior of reference and aged CF/PEKK samples: (a) Stress-strain curves and, (b) Bar chart of maximum compressive strength, before and after reconsolidation.

the fracture behavior. Despite the increased strength of the Reference_AA samples, delamination in the central region is more severe compared to the Reference_BA sample (Figure 9(c)). The delamination between the layers has increased, and fiber fractures are observed. Additionally, the outer 45° layers have completely pulled out. This is attributed to the weakening of the interface with aging, which facilitates fiber-matrix debonding through swelling and increased interlayer delamination.[9] In contrast, the delamination between layers is reduced, and fiber pull-out is less pronounced in the Reconsolidate_AA samples, which have a decreased compressive strength of (569.46 ± 13.78) MPa after reconsolidation (Figures 8(b) and 9(d)). The reduction in compressive strength is linked to the reconsolidation process, where controlled heat and pressure applied during hot-pressing recover the effects of hydrothermal aging. This is supported by the fact that the compressive strength of the reconsolidated samples is nearly the same as before.

Given that drilling is an integral process in the production of aircraft components, it is essential to comprehensively understand the behavior of drilled samples under compressive loading. To this end, open hole compression tests are conducted in accordance with ASTM D6484. The stress-strain curves obtained from these tests are illustrated in Figure 10. The open hole compressive strengths of the reference and reconsolidated CF/PEKK samples are determined to be (233.87 ± 10.01) MPa and (322.62 ± 6.29) MPa, respectively (Figure 10(a)). Moreover, the strain values increased by 29.3%. It is believed that reconsolidation relieves residual stresses in the matrix, thereby enhancing both the stiffness and toughness of the CF/PEKK samples. This improvement is observed in open hole compression tests and is also applicable to compression tests (Figures 8(a) and 10(a)).[60] Furthermore, from the images in Figure 11(a), minor delamination is observed around the hole following the drilling process. The stress concentration around the hole
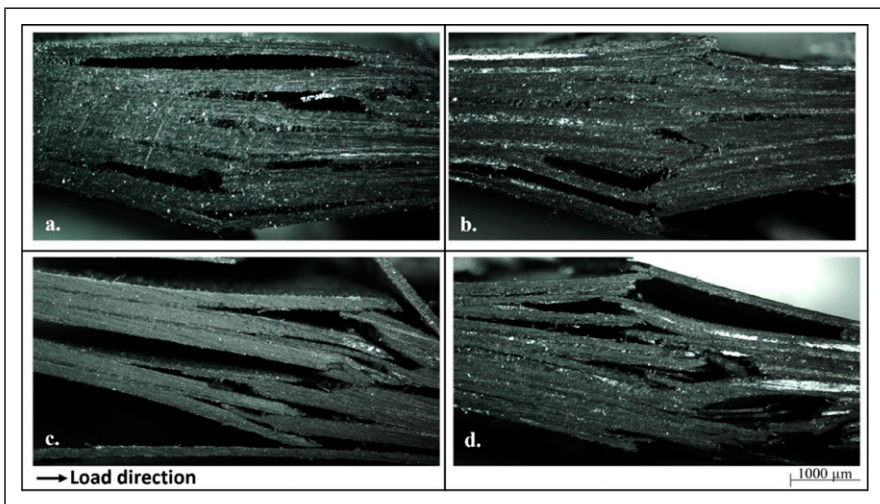

Figure 9. Optical microscopy images of compression samples after test, (a) Reference_BA, (b) Reconsolidate_BA, (c) Reference_AA, (d) Reconsolidate_AA.
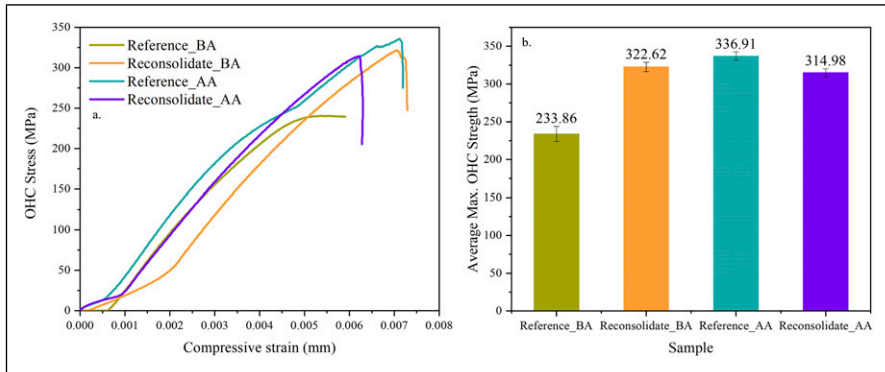
Figure 10. OHC behavior of reference and aged CF/PEKK samples: (a) Stress-strain curves and (b) Bar chart of maximum compressive strength, before and after reconsolidation.
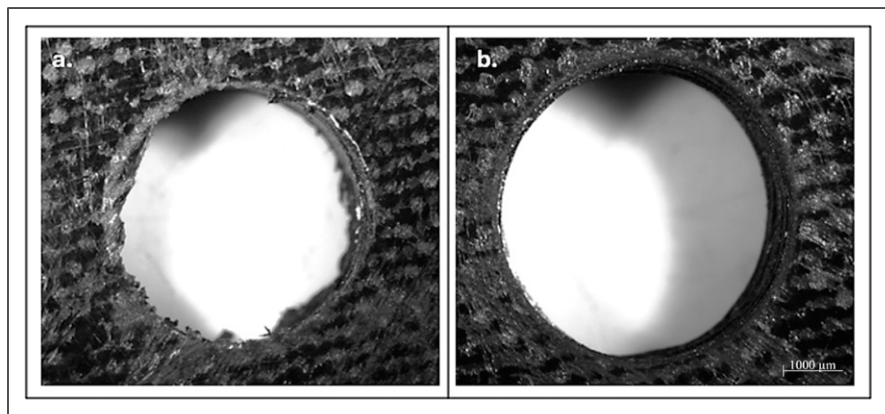

Figure 11. Optical microscopy images of the sample around the hole (a) After drilling, (b) After reconsolidation.

may result in a reduced resistance under load.[61] However, reconsolidation following drilling visibly improves surface quality, particularly around the hole, which correlates with increased OHC strength. Failure occurred in a similar manner in Reference_BA and Reconsolidate_BA samples, with cracks forming perpendicular to the direction of the applied load and propagating along the width of the sample (Figure 12(a) and (b)).

It is observed that following the hot aging process, both the open hole compressive strength and strain values exhibit a trend similar to the increase in overall compressive strength. The open hole compressive strength increases from (233.87 ± 10.01) MPa (Reference_BA, Figure 10(a)) to (336.91 ± 5.51) MPa (Reconsolidate_AA, Figure 10(b)). It is believed that high temperatures and water exposure during aging cause post-crystallization reaction in the matrix and reduce residual stresses from the laminate.

The absorbed water likely acts as a plasticizer for the polymer matrix, facilitating the alleviation of residual stresses within the material.[26,27,62,63] However, despite the increase in strength value, the sample fractured into two pieces along the perpendicular axis of the applied load direction as seen in Figure 12(c). As stated above, when water molecules penetrating composite samples can weaken the fiber-matrix interface, promoting fiber to detachment due to swelling, and causing more catastrophic failure. A similar trend are observed in the strength values of reconsolidated open hole samples at the end of the aging period. The strength value of Reconsolidate_AA sample is decreased to (314.98 ± 5.30) MPa compared to Reference_AA (Figure 10(b)). Fortunately, with reconsolidation, the catastrophic detachment failure is recovered (Figure 12(d)) and the failure is similar to Reference_BA and Reconsolidate_BA samples.

The compressive properties of the compression and open hole compression samples after reconsolidation (Reconsolidate_AA and Reconsolidate_BA) are nearly identical. This suggests that the reconsolidation process effectively removes absorbed water and restores the physical changes in the polymer matrix that occurred during the aging period. The decrease in average mass and other analyses corroborate the conclusions drawn from the mechanical tests. A similar phenomenon has been reported in the literature; for instance, Bel Haj Frej et al.[64] documented a recovery in the tensile properties of acrylic thermoplastic composites after drying following an aging period at 40°C. Additionally, the reconsolidation process aids in repairing damage incurred during machining by applying controlled heat and pressure. Residual stresses in thermoplastic composites are relieved through reconsolidation due to the thermal history and processing conditions. During reconsolidation, the heating and cooling phases can lead to the relaxation or redistribution of residual stresses. The observed increase in strength and improvement in failure behavior of samples after aging are attributed to this stress relaxation.[65]
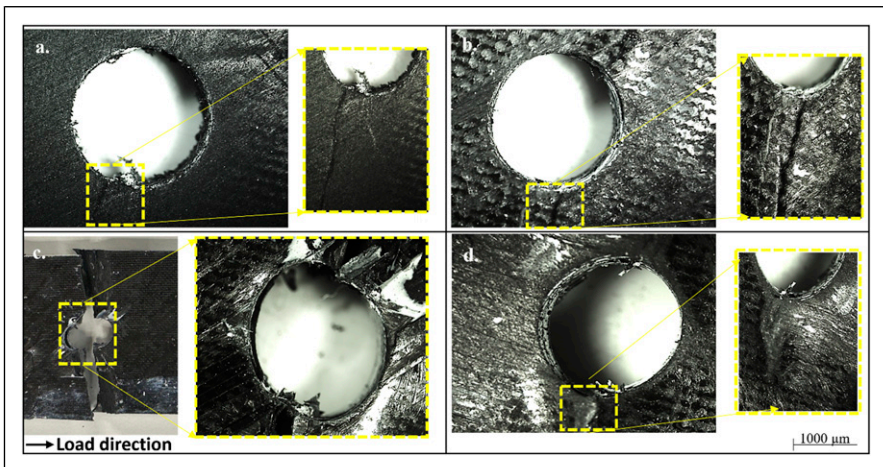

Figure 12. Optical microscopy images of open hole compression samples after test: (a) Reference_BA, (b) Reconsolidate_BA, (c) Reference_AA, and (d) Reconsolidate_AA.

Digital image correlation (DIC) Inspection

To comprehensively understand the effect of reconsolidation, mechanical tests are supported by DIC which is a non-contact optical method that provides full-field strain measurements, allowing for precise monitoring of strain distribution and deformation patterns in the samples.[66] This technique enables the identification of strain relief and redistribution due to the controlled heat and pressure applied during the reconsolidation process. Figure 13 presents the compressive (right) and shear (left) strain maps of the compression samples at maximum load values. A non-uniform compressive and shear strain distribution is observed in the Reference_BA sample indicating insufficient load transfer under compressive loading. This is also implied by the delamination-dominated failure of Reference_BA sample as shown in Figure 9(a). In contrast, a more homogenous compressive and shear strain distributions are observed for the Reconsolidate_BA sample. It is clear that the reconsolidation process eliminates residual stresses occurred during the manufacturing process, leading to enhanced damage resistance and higher, compressive strength and strain values compared to Reference_BA sample with less catastrophic delamination as seen in Figure 8(b).

In the Reference_AA sample, shear and compressive strain areas are increased compared to their unaged counterparts. As mentioned in the previous section, a small amount of water entering the composite sample during aging has a plasticizer effect, which causes non-uniform strain distribution and leads to higher compressive performance. However, delamination is more prominent as seen in Figure 8(c). Thus, the strain distribution is more balanced after reconsolidation in Reconsolidated_AA samples. Additionally, the strain distribution becomes more uniform, guesting the removal of
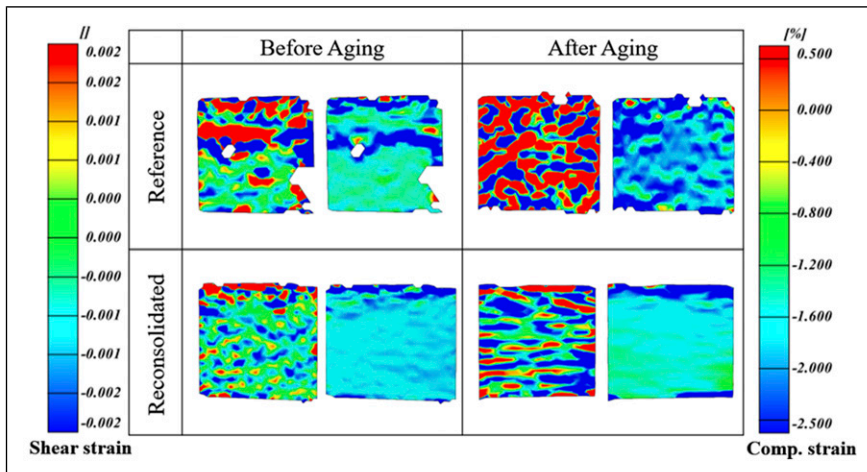

Figure 13. Full field strain distribution of compression samples at maximum load for reference and reconsolidated samples before and after aging.

absorbed moisture, which agrees with the weight change results (Figure 4) and indicates improved bonding quality with reconsolidation.[67]

The compressive strain (right) and shear strain (left) distribution maps of OHC samples at maximum load values are displayed in Figure 14. High compressive and tensile strain regions at the circumference of the hole are observed in all samples. In the Reference_BA sample, the high compressive strain regions are not aligned perpendicular to the loading direction, indicating inadequate load transfer around the periphery of the hole. This is also apparent in the shear strain distribution map, where the shear strains and stresses are not spread evenly over the sample. In contrast, the high compressive strain regions in the Reconsolidated_BA sample are aligned perpendicularly to the loading direction, and the shear strains are widespread across the sample. This behavior can be attributed to the reconsolidation process enhancing the perforation surface, as seen in Figure 11. Moreover, the improvement in strain distribution also enhances the failure behavior, as delamination is diminished, as seen in Figure 12(b).

After the aging period, it is observed that the high compressive strain regions are less tilted with respect to loading direction in the Reference_AA sample compared to those in the Reference_BA. This indicates that the aging process facilitates efficient load distribution around the hole by closing the microcracks formed during drilling, hence resulting in improved compressive strength compared to the reference counterpart. However, the water leads localized strain areas, weakening the interface between fiber and matrix, and consequently causing catastrophic failure (Figure 12(c)). The shear strain distribution is more balanced in the OHC sample after reconsolidation, suggesting a reduction in localized shear deformation. Consequently, recovery in the delamination behavior (Figure 12(d)).
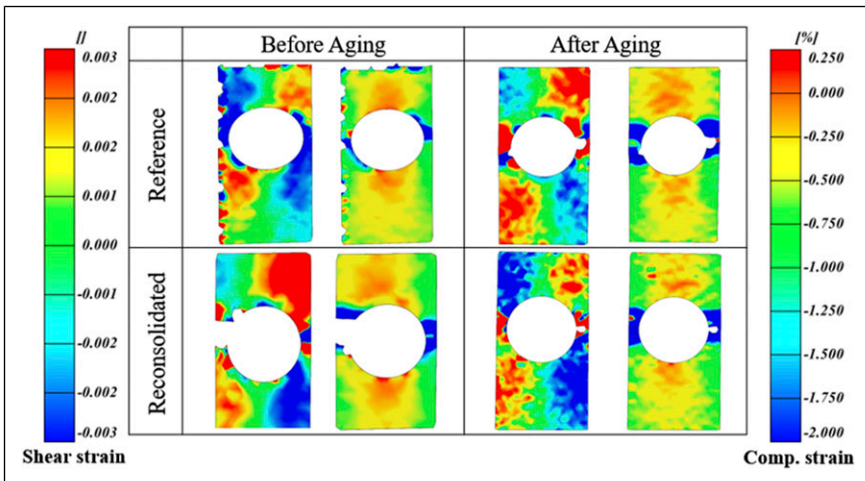

Figure 14. Full field strain distribution of open hole compression samples at maximum load for reference and reconsolidated samples before and after aging.

In summary, the reconsolidation process effectively restores CF/PEKK composites by mitigating drilling damage and hydrothermal aging, improving mechanical performance and reducing moisture absorption based on the results. However, certain limitations should be considered when ensuring uniform heat and pressure distribution for the repair of large structures. Processing methods tailored for this purpose should be developed. Among existing manufacturing techniques, thermoforming can also be considered a potential candidate for this application, which involves a three-stage process, heating the material blank with thermal deconsolidation, followed by part forming and re-consolidation in a matched tool,[68] overcomes certain limitations regarding large scale applications. However, repeated reconsolidation cycles may lead to cumulative aging effects, such as increased brittleness or microcracking. Despite these limitations, it re-mains a promising method for extending composite durability.

Conclusion

This study demonstrates the effect of reconsolidation in improving the mechanical properties and structural integrity of CF/PEKK composites subjected to drilling and hot-wet aging. The application of heat and pressure during the reconsolidation process significantly mitigate the damages caused by drilling and hydrothermal aging. The re-consolidated samples exhibit enhanced mechanical properties, with compressive strength increased by 15.61% in compression samples and by 37.61% in OHC samples before aging. Moreover, reconsolidation effectively recovers the catastrophic effects of aging. DIC results reveal that the reconsolidation process effectively restored the deformation characteristics of the material to near initial states, as evidenced by the more uniform strain distribution in reconsolidated samples. This indicates a reduction in stress con-centrations that typically lead to premature failure. Furthermore, thermal analysis indi-cates a notable increase in the glass transition temperature, T_g, and degree of crystallinity, X_c, in the reconsolidated samples, supporting the mechanical analysis results. Specifi-cally, in samples before aging, X_c and T_g increased by 20.94% and 5.97%, respectively. Overall, the findings of this study suggest that reconsolidation offers a promising solution for maintaining the structural and functional integrity of CF/PEKK composites in aerospace and other high-performance applications. Further studies are required to evaluate the durability of reconsolidated composites under extended service conditions and repeated repair cycles to overcome the limitations.

Author contributions

Sinem Elmas: Conceptualization (equal); data curation (lead); methodology (equal); validation (lead); visualization (lead); writing – original draft (lead); writing – review and editing (equal). Buse Atac: Conceptualization (equal); methodology (equal); writing – original draft (supporting); writing – review and editing (supporting). Abdulrahman Al-Nadhari: Data curation (lead); visu-alization (supporting); writing – original draft (supporting). Serra Topal: Conceptualization (equal); funding acquisition (equal); methodology (equal); methodology (equal). Mehmet Yildiz: Funding acquisition (equal); writing – review and editing (supporting). Hatice S. Sas: Conceptualization

(equal); funding acquisition (lead); methodology (lead); supervision (lead); writing – review and editing (equal).

Declaration of conflicting interests

Funding

ORCID iD

Hatice S Sas https://orcid.org/0000-0002-5179-2509

Data Availability Statement

Data will be made available on request.

Supplemental Material

Supplemental material for this article is available online.

References

1. Bajurko P. Comparison of damage resistance of thermoplastic and thermoset carbon fibre-reinforced composites. *J Thermoplast Compos Mater* 2021; 34: 303–315.
2. Bhudolia SK, Gohel G, Leong KF, et al. Advances in ultrasonic welding of thermoplastic composites: a review. *Materials* 2020. https://www.mdpi.com/1996-1944/13/6/1284/htm
3. Arquier R, Iliopoulos I, Régnier G, et al. Consolidation of continuous-carbon-fiber-reinforced PAEK composites: a review. *Mater Today Commun* 2022; 32: 104036.
4. Pérez-Martín H, Mackenzie P, Baidak A, et al. Crystallinity studies of PEKK and carbon fibre/PEKK composites: a review. *Composites Part B* 2021; 223: 109127.
5. Ramaswamy K, Modi V, Rao PS, et al. An investigation of the influence of matrix properties and fibre–matrix interface behaviour on the mechanical performance of carbon fibre-reinforced PEKK and PEEK composites. *Compos Part A Appl Sci Manuf* 2023; 165: 107359.
6. Zhang D, Heider D and Gillespie JW. Void reduction of high-performance thermoplastic composites via oven vacuum bag processing. *J Compos Mater* 2017; 51: 4219–4230.
7. Zhang D, Heider D and Gillespie JW. Design and optimization of oven vacuum bag (OVB) processing for void air removal in high-performance thermoplastic composites. *J Thermoplast Compos Mater* 2020; 35: 2493–2511.

8. Swamy JN, Grouve WJ, Wijskamp S, et al. An experimental study on the role of different void removal mechanisms in VBO processing of advanced thermoplastic composites. *J Reinforc Plast Compos* 2024; 43(3–4): 183–194.

9. Sukur EF, Elmas S, Seyyednourani M, et al. A rational study on the hydrothermal aging of AFP manufactured CF/polyetherketoneketone composites with in situ consolidation supported by acoustic emission inspection. *J Appl Polym Sci* 2022; 139: 1–14.

10. Xu J, Yin Y, Paulo Davim J, et al. A critical review addressing drilling-induced damage of CFRP composites. *Compos Struct* 2022; 294: 115594.

11. Durão LMP, Tavares JMRS, de Albuquerque VHC, et al. Drilling damage in composite material. *Materials* 2014; 7: 3802–3819.

12. Ge J, Catalanotti G, Falzon BG, et al. Process characteristics, damage mechanisms and challenges in machining of fibre reinforced thermoplastic polymer (FRTP) composites: a review. *Compos B Eng* 2024; 273: 111247.

13. Ge J, Fu G, Almeida Jr JHS, et al. Thermal effect in CFRP machining: temperature field characteristics, heat generation mechanism and thermal damage management. *Compos Struct* 2025; 356: 118845.

14. Ge J, Zhang W, Luo M, et al. Multi-objective optimization of thermoplastic CF/PEKK drilling through a hybrid method: an approach towards sustainable manufacturing. *Compos Part A Appl Sci Manuf* 2023; 167: 107418.

15. Ge J, Catalanotti G, Falzon BG, et al. Towards understanding the hole making performance and chip formation mechanism of thermoplastic carbon fibre/polyetherketoneketone composite. *Composites Part B* 2022; 234: 109752.

16. Naebe M, Abolhasani MM, Khayyam H, et al. Crack damage in polymers and composites: a review. *Polym Rev* 2016; 56: 31–69.

17. Sukur EF, Elmas S, Seyyednourani M, et al. Effects of meso- and micro-scale defects on hygrothermal aging behavior of glass fiber reinforced composites. *Polym Compos* 2022; 43: 8396–8408.

18. Katnam KB, Da Silva LFM and Young TM. Bonded repair of composite aircraft structures: a review of scientific challenges and opportunities. *Prog Aero Sci* 2013; 61: 26–42.

19. Budhe S, Banea MD and de Barros S. Bonded repair of composite structures in aerospace application: a review on environmental issues. *Appl Adhes Sci* 2018; 6: 3.

20. Shetty K, Bojja R and Srihari S. Effect of hygrothermal aging on the mechanical properties of IMA/M21E aircraft-grade CFRP composite. *Adv Compos Lett* 2020; 29: 1–9.

21. Barkoula N.-M. Environmental Degradation of Carbon Nanotube Hybrid Aerospace Composites. In: Paipetis A. and Kostopoulos V. (eds) *Carbon Nanotube Enhanced Aerospace Composite Materials. Solid Mechanics and Its Applications*. Dordrecht: Springer, 2013, 188, pp. 337–376.

22. Alessi S, Pitarresi G and Spadaro G. Effect of hydrothermal ageing on the thermal and de-lamination fracture behaviour of CFRP composites. *Composites Part B* 2014; 67: 145–153.

23. Borba NZ, dos Santos JF and Amancio-Filho ST. Hydrothermal aging of friction riveted thermoplastic composite joints for aircraft applications. *Compos Struct* 2021; 255: 112871.

24. Shah CS and Panti MJ. Accelerated aging and life time prediction analysis of polymer composites: a new approach for a realistic prediction using cumulative damage theory. *Polymer testing* 1994; 13(4): 295–322.

25. Batista NL, Rezende MC and C Botelho E. The influence of crystallinity on the weather resistance of CF/PEEK composites. *Appl Compos Mater* 2021; 28: 235–246.

26. Mazur RL, Cândido GM, Rezende MC, et al. Accelerated aging effects on carbon fiber PEKK composites manufactured by hot compression molding. *J Thermoplast Compos Mater* 2016; 29: 1429–1442.

27. Sukur EF, Elmas S, et al. An experimental implication of long-term hot-wet-aged carbon fiber/polyether ketone ketone composites: the impact of automated fiber placement process parameters and process-induced defects. *J Appl Polym Sci* 2023; 140(29): e54076.

28. Erland S, Stevens H and Savage L. The re-manufacture and repairability of poly(ether ether ketone) discontinuous carbon fibre composites. *Polym Int* 2021; 70: 1118–1127.

29. Ragupathi B, Bacher MF and Balle F. First efforts on recovery of thermoplastic composites at low temperatures by power ultrasonics. *Clean Mater* 2023; 8: 100186.

30. Conejo LS, Santos LFd. P, Ribeiro B, et al. Reconsolidation effect on impact, compression after impact and thermal properties of poly (aryl ether ketone) composites for aeronautical applications. *J Thermoplast Compos Mater* 2023; 36: 2562–2581.

31. Parlevliet PP, Bersee HEN and Beukers A. Residual stresses in thermoplastic composites-A study of the literature-Part I: formation of residual stresses. *Compos Part A Appl Sci Manuf* 2006; 37: 1847–1857.

32. Lebrun G and Denault J. Effect of annealing on the thermal expansion and residual stresses of bidirectional thermoplastic composite laminates. *Compos Part A Appl Sci Manuf* 2010; 41: 101–107.

33. Erkliğ A, Abidin Oğuz Z and Bozkurt Y. An experimental investigation on the charpy impact response of glass/epoxy composites aged in seawater. *Int J Mater Eng Technol* 2021; 004: 51–60.

34. Borba NZ, Kötter B, Fiedler B, et al. Mechanical integrity of friction-riveted joints for aircraft applications. *Compos Struct* 2020; 232: 111542.

35. Karimi S, Louyeh PY, et al. A study of post-processing for AFP-fabricated thermoplastic composites with void content and air permeability characterization. *J Reinforc Plast Compos* 2023; 43(9–10): 490–503.

36. Elkolali M, Nogueira LP, Rønning PO, et al. Void content determination of carbon fiber reinforced polymers: a comparison between destructive and non-destructive methods. *Polym* 2022; 14: 1212.

37. Hexcel Corporation. HexTow® AS4 – carbon fiber. Data sheet, 2023, 4–6.

38. Toray Cetex ® TC1320 PEKK PRODUCT DATA SHEET PRODUCT TYPE PEKK (PolyEtherKetoneKetone). 2022, 3–5.

39. Ge J, Luo M, Zhang D, et al. Temperature field evolution and thermal-mechanical interaction induced damage in drilling of thermoplastic CF/PEKK – a comparative study with thermoset CF/epoxy. *J Manuf Process* 2023; 88: 167–183.

40. Amedewovo L, Levy A, de Parscau du Plessix B, et al. A methodology for online characterization of the deconsolidation of fiber-reinforced thermoplastic composite laminates. *Compos Part A Appl Sci Manuf* 2023; 167: 107412.

41. Fink BK, Gillespie JW and Ersoy NB. *Thermal degradation effects on consolidation and bonding in the thermoplastic fiber-placement process*. Adelphi, MD, USA: Army Research Laboratory, 2000.

42. Hoang V-T, Kwon B-S, et al. Postprocessing method-induced mechanical properties of carbon fiber-reinforced thermoplastic composites. *J Thermoplast Compos Mater* 2020; 36(1): 432–447.

43. Liu A, Chen Y, et al. Low-velocity impact damage and compression after impact behavior of CF/PEEK thermoplastic composite laminates. *Polymer Composites* 2022; 43(11): 8136–8151.

44. Quiroga Cortés L, Caussé N, Dantras E, et al. Morphology and dynamical mechanical properties of poly ether ketone ketone (PEKK) with meta phenyl links. *J Appl Polym Sci* 2016; 133: 1–10.

45. Ghiorse SR. Effect of void content on the mechanical properties of carbon/epoxy laminates. *SAMPE Quarterly* 1993; 24(2): 54–59.

46. Friedrich K, Fakirov S and Zhang Z. Polymer composites: from nano- to macro-scale 2006.

47. Wang X, Hou Z and Yang Y. A study on the aging resistance of injection-molded glass fiber thermoplastic composites. *Fibers Polym* 2022; 23: 502–514.

48. Slange TK, Warnet LL, Grouve WJB, et al. Deconsolidation of C/PEEK blanks: on the role of prepreg, blank manufacturing method and conditioning. *Compos Part A Appl Sci Manuf* 2018; 113: 189–199.

49. Ostberg GMK and Seferis JC. Annealing effects on the crystallinity of polyetheretherketone (PEEK) and its carbon fiber composite. *J Appl Polym Sci* 1987; 33: 29–39.

50. Elmas S, Atac B, Senol CO, et al. Annealing impact on mechanical performance and failure analysis assisted with acoustic inspection of carbon fiber reinforced poly-ether-ketone-ketone composites under flexural and compressive loads. *Polymer Composites* 2025; 46(4): 3686–3704. DOI: 10.1002/pc.29199, In this issue.

51. Martin RG, Johansson C, Tavares JR, et al. Manufacturing of thermoplastic composite sandwich panels using induction welding under vacuum. *Compos Part A Appl Sci Manuf* 2024; 182: 108211.

52. Vasconcelos GC, Mazur RL, Ribeiro B, et al. Evaluation of decomposition kinetics of poly (ether-ether-ketone) by thermogravimetric analysis. *Mat Res* 2013; 17: 227–235.

53. Iggui K, Kaci M, Le Moigne N, et al. Effects of hygrothermal aging on chemical, physical, and mechanical properties of poly(3-hydroxybutyrate-co-3-hydroxyvalerate)/Cloisite 30B bionanocomposite. *Polym Compos* 2021; 42: 1878–1890.

54. Menard KP. *Dynamic Mechanical Analysis*. 2nd ed. CRC Press, 2008.

55. Meng Q, Gu Y, Luo L, et al. Annealing effect on crystalline structure and mechanical properties in long glass fiber reinforced polyamide 66. *J Appl Polym Sci* 2017; 134: 1–10.

56. Amash A and Zugenmaier P. Thermal and dynamic mechanical investigations on fiber-reinforced polypropylene composites. *Journal of Applied Polymer Science* 1997; 2863(9): 1143–54.

57. Manap A, Mahalingam S, Vaithylingam R, et al. Mechanical, thermal and morphological properties of thermoplastic polyurethane composite reinforced by multi-walled carbon nanotube and titanium dioxide hybrid fillers. *Polym Bull* 2021; 78: 5815–5832.

58. Sanders B, Cant E, Amel H, et al. The effect of physical aging and degradation on the Re-use of polyamide 12 in powder bed fusion. *Polymers* 2022; 14(13): 2682.

59. Farhoodi M, Mousavi SM, Sotudeh-Gharebagh R, et al. A study on physical aging of semicrystalline polyethylene terephthalate below the glass transition point. *J Appl Res Technol* 2012; 10: 698–702.

60. Liu A, Zou Y, Chen Y, et al. Experimental investigation of impact resistance and compression behavior of CF/PEEK laminates after hot-press fusion repair with different stacking sequences 2023: 6467–6481.

61. Campos Rubio J, Abrao AM, Faria PE, et al. Effects of high speed in the drilling of glass fibre reinforced plastic: evaluation of the delamination factor. *Int J Mach Tool Manufact* 2008; 48: 715–720.

62. Cysne Barbosa AP, Ana AP, Guerra E SS, et al. Accelerated aging effects on carbon fiber/epoxy composites. *Composites Part B* 2017; 110: 298–306.

63. Marouani S, Curtil L and Hamelin P. Ageing of carbon/epoxy and carbon/vinylester composites used in the reinforcement and/or the repair of civil engineering structures. *Composites Part B* 2012; 43: 2020–2030.

64. Bel Haj Frej H, Léger R, Perrin D, et al. Effect of aging temperature on a thermoset-like novel acrylic thermoplastic composite for marine vessels. *J Compos Mater* 2021; 55: 2673–2691.

65. Wang Y and Wu Q. A microscale analysis of thermal residual stresses in composites with different ply orientations. *Mater* 2023; 16: 6567.

66. Yildirim C, Tabrizi IE, Al-Nadhari A, et al. Characterizing damage evolution of CF/PEKK composites under tensile loading through multi-instrument structural health monitoring techniques. *Compos Part A Appl Sci Manuf* 2023; 175: 107817.

67. Zacherl L, Shadmehri F and Rother K. Determination of convective heat transfer coefficient for hot gas torch (HGT)-assisted automated fiber placement (AFP) for thermoplastic composites. *J Thermoplast Compos Mater* 2023; 36: 73–95.

68. Han P, Butterfield J, Price M, et al. Experimental investigation of thermoforming carbon fibre-reinforced polyphenylene sulphide composites. *J Thermoplast Compos Mater* 2015; 28: 529–547.